Demystifying the Ferrocell

Preprint · November 2021

CITATIONS
0

READS
1,754

1 author:

Lori Gardi
Western University
80 PUBLICATIONS **1,015** CITATIONS

SEE PROFILE

Demystifying the Ferrocell

L. Gardi

Senior Software Developer, Western University, London, Ontario, Canada

November 21, 2021

1 Abstract

The Ferrocell is an optical viewing device that interacts with a magnetic field and one or more light sources to produce a real-time visual light display. Although this display has been historically shrouded in mystery, the actual explanation is quite simple. Using numerical methods and known physical laws, we show how the light patterns as seen in the Ferrocell are primarily caused by light reflections off the magnetic needle-like filaments that form and align along magnetic flux lines in the presence of a magnetic field.

2 Introduction

A ferrolens is best described as a Hele-Shaw cell (two closely spaced parallel plates with fluid between them). In a typical ferrolens, a ferrofluid mixture is sandwiched between two optically flat pieces of glass. The visual effects appear when a magnet is placed in the vicinity of the lens that is illuminated with one or more light sources. Tufaile et el have identified these "visual effects" as being caused by reflection analogous to what happens in atmospheric optics, [1][2]. Thus, in our simulations, the law of reflection is used as the starting point. Since "what the observer sees" is highly dependent on the position of the magnet, the lights, and the observer (with respect to the ferrolens), all of these parameters were taken into consideration in the simulation. The results of the simulations show that reflection is the primary cause of the patterns as seen in ferrolens, and scattering is responsible for the fuzziness of the patterns (as one would expect of any optical device). Here, scattering is defined as a deviation from the ideal path of the reflected light. In the research presented herein, numerical methods and computer simulations were used to model a variety of magnetic configurations and ferrolens displays.

3 Scope

The simulations presented in this paper are limited to the thin layer of ferrous particles sandwiched between the two pieces of glass and do not incorporate the effects of the glass itself or the fluid mixture. The purpose of this research was to build a simulation that accurately predicts (and reproduces) the patterns that the observer sees when looking at a Ferrocell.

4 Background

Ferrofluid is a colloidal solution of magnetic nano-particles suspended in a carrier fluid such as water or some other organic solvent. Each nanoparticle (around 10 nm in size) consists of a ferrimagnetic or ferromagnetic core coated with a surfactant (eg. oleic acid) to inhibit aggregation. In the ferrolens, the ferrofluid is further diluted using some lubricant (eg. WD-40, mousemilk, baby oil) and placed in a thin layer between two pieces of optically flat glass or some other transparent material.

Upon application of an external magnetic field, the nanoparticles in the ferrolens self-organize into needle-like filaments which are in the order of 100 micrometers in length [5]. These micro-needles then align with the magnetic field to minimise dipolar interactions as seen under the microscope in Figure 1. The light from the light source (LED, laser etc.) reflects off these filaments and into the eye (or camera) to produce interesting patterns that change in real-time as the magnet is moved around.

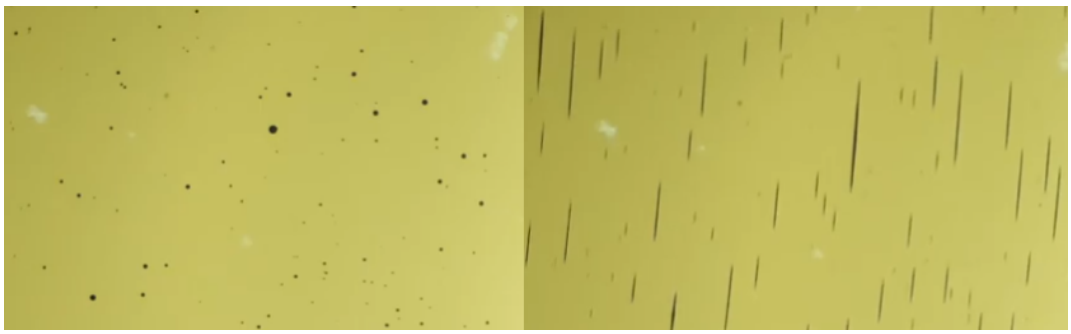

Figure 1: Ferrolens under a microscope. Left: Ferrofluid in the absence of a magnet. Right: Ferrofluid in the presence of a magnet. Longer filaments in the order of 100 microns in length.

Specular reflections are described by the law of reflection giving the reflection vector ($\mathbf{R}$) as a function of the incident vector ($\mathbf{I}$) and the surface normal vector ($\hat{\mathbf{N}}$) at the reflection point, with the constraint that $\mathbf{I} \cdot \hat{\mathbf{N}} < 0$.

$$\mathbf{R} = \mathbf{I} - 2(\mathbf{I} \cdot \hat{\mathbf{N}})\hat{\mathbf{N}} \tag{1}$$

It is well known that light striking a thin edge results in an optical phenomenon know as a Keller's cone [3]. A Keller's cone can also be described as all valid reflection values of $\mathbf{R}$ for light striking an extremely thin cylinder at some angle θ without the aforementioned constraint. Keller's geometric diffraction theory extends beyond the concepts of reflection and refraction with the addition of diffraction [4]. For a thin cylinder, incident light is also diffracted around the obstruction producing interference patterns as noted by Tufaile et al [5]. The simulation presented in this paper is primarily targeting Keller's cone and not the interference patterns which contribute minimally to the light patterns seen in the ferrolens.

We can consider the needle-like filaments that form upon application of a magnetic field as micro-cylinders with the long axis aligned with the magnetic field. Incident light reflects off the cylinders and when the observer's eye intersects the resultant Keller cone, the observer will perceive a bright spot. Some deviations from the predicted reflections (scattering) is also involved. From this, we see that the lines observed in the ferrolens are all the points where (1) holds without the constraint that $\mathbf{I} \cdot \hat{\mathbf{N}} < 0$. Here, $\mathbf{I}$ is the displacement vector from a light to the micro-cylinders, and $\mathbf{R}$ is the displacement vector from the cylinders to the observer's eye.

5 Methods

5.1 Experimental

The ferrolens (Hele-Shaw cell) used in these experiments was created using 2 optically flat glass disks. A few drops of a fluid mixture consisting of 1 part ferrofluid (EFH series) to 1 part baby oil is placed in the center of the first glass disk. The second glass disk is then placed on top of the first causing the fluid to spread between the two pieces of glass. The optical flatness of the glass allows for a very thin layer to form, in the order of 10 microns. A magnet or set of magnets is then placed under the ferrolens and one or more light sources are used to illuminate the lens. A camera is positioned above the ferrolens to capture the patterns that form when the magnet is in place.

5.2 Simulation

The simulation starts with a structured grid of $x, y, z = 0$ coordinates to represent position vectors $\mathbf{p}$ within the ferrolens film. Given a magnet or set of magnets of specific geometry, the magnetic field is then computed with arbitrary units by defining a 3D structured grid with position $\mathbf{q}$ and normalised magnetic moment $\hat{\mu}$ such that the field at a given point is the sum of the field due to each moment in the magnet,

$$\mathbf{B}(\mathbf{p}) = \sum_i \frac{1}{r_i^3}[\hat{\mu} - 3(\hat{\mathbf{r_i}} \cdot \hat{\mu})\hat{\mathbf{r_i}}] \tag{2}$$

where $r_i = \mathbf{p} - \mathbf{q_i}$. The direction of each micro-cylinder's long axis is then given by the unit vector $\hat{\mathbf{B}}$ at position $\mathbf{p}$. For simplicity, a software package called Magpylib is utilized for these calculations [7]. The positions of the lights are then taken into consideration $\mathbf{L}$, as well as the position of the observer $\mathbf{o}$. With known incident and reflection vectors, the normal vector is recovered in equation 1 by normalising the difference between the reflection vector and incident vector:

$$\hat{\mathbf{N}} = \frac{\mathbf{R} - \mathbf{I}}{|\mathbf{R} - \mathbf{I}|} \tag{3}$$

To calculate the normal vector, $\hat{\mathbf{N}}$, the incident vector $\mathbf{I} = \mathbf{p} - \mathbf{L}$ and reflection vector $\mathbf{R} = \mathbf{o} - \mathbf{p}$ are substituted into equation 3. To be consistent with equation 1, the condition $\hat{\mathbf{B}} \cdot \hat{\mathbf{N}} = 0$ must hold for a point $\mathbf{p}$ to appear illuminated to the observer. Since numerical methods are limited in precision, it is unlikely that a simulation would return a situation where these conditions hold. However, the micro-cylinders in an experimental system have finite roughness and not a perfect circular cross-section. In addition, the light sources and the observer are not point-like. These imperfections allow us to relax the condition such that a point is considered illuminated if $|\hat{\mathbf{B}} \cdot \hat{\mathbf{N}}| < T$ where T represents some threshold value to expand the range with which we can consider the result valid. This can be considered as a first order implementation of scattering.

6 Results

Figure 2 shows how a single light source interacts with the ferrolens in the presence of a magnet. The simulation (middle image) is calibrated to the experimental setup on the left as specified in this figure. Here you will notice that the loop of light appears to intersect a point at the center of the LED. This is the light source that that is being targeted in the simulation. The light emitted at

the front and back ends of the LED are not being simulated as they do not contribute significantly to the light patterns seen in the ferrolens. As you can see, the curved light line predicted by the simulation accurately matches the curve as seen in the ferrolens.

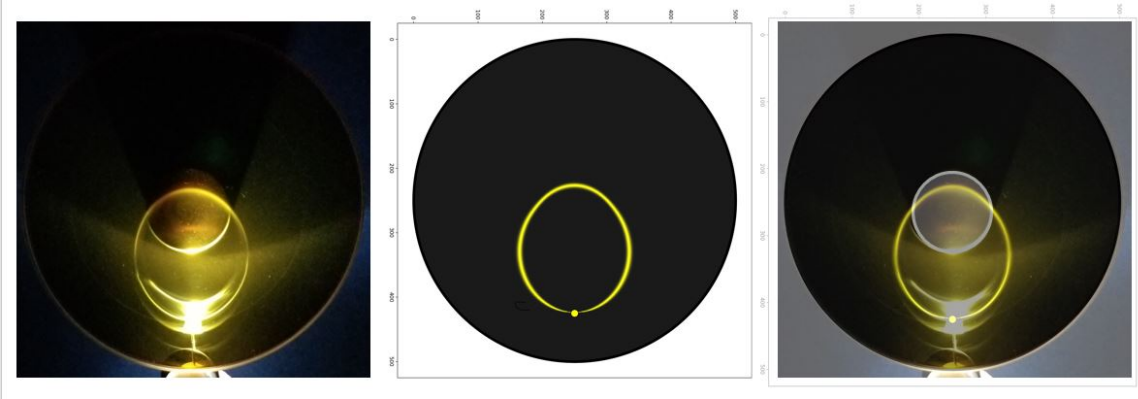

Figure 2: Left: Cylinder magnet (d=20mm, h=25mm) under a 10cm diameter ferrolens. Polar view. A single white LED light source is used to illuminate the ferrolens. Middle: Simulation of experimental setup. Right: Experiment and simulation merged together. Magnet highlighted.

In Figure 3, there are 36 lights (red, green, blue and yellow) surrounding a 5cm diameter ferrolens with a cylinder magnet in polar view (N-pole up) under the lens. The simulation on the right is calibrated to the experimental setup on the left. The magnet is highlighted in grey. Notice that the central black region in the simulation does not correspond to the outer boundary of the magnet. Instead, it corresponds to a smaller darker circular region in the center of the magnet as can be seen in the ferrolens image. As you can see, the simulation accurately predicts the trajectories of the curved light lines as well as the central dark region as seen in Figures 2 and 3.

In figure 4 there are 36 lights (white only) surrounding a 10cm diameter ferrolens. A large cube magnet is placed under the ferrolens in a dipole orientation (poles are to the left and right). The simulation on the right is calibrated to the experimental setup on the left. In this simulation, you can see that the light lines match very well to what is seen in the ferrolens as well as the locations and shapes of the dark voids near either pole.

In figure 5 there are 36 lights (red, green blue and white) surrounding a 5cm diameter ferrolens with two cylinder magnets in a quadrapole configuration. As usual, the simulation on the right is calibrated to the experimental setup on the left. As you can see, the correlation between the experimental setup and the simulation is quite good. In the simulation however, you may notice some artifacts in the image that are not seen in the ferrolens. This problem was fixed by placing a thin black barrier between the magnet and the ferrolens thus hiding the magnet from view. Also, since we are not simulating the effects of the glass, the top glass disk was removed from the ferrolens. After removing the glass and hiding the magnet, the extra features seen in the simulation were also seen in the ferrolens as can be seen in Figure 6. This was a good test of the algorithm as it was able to make a prediction that was subsequently proven by experiment.

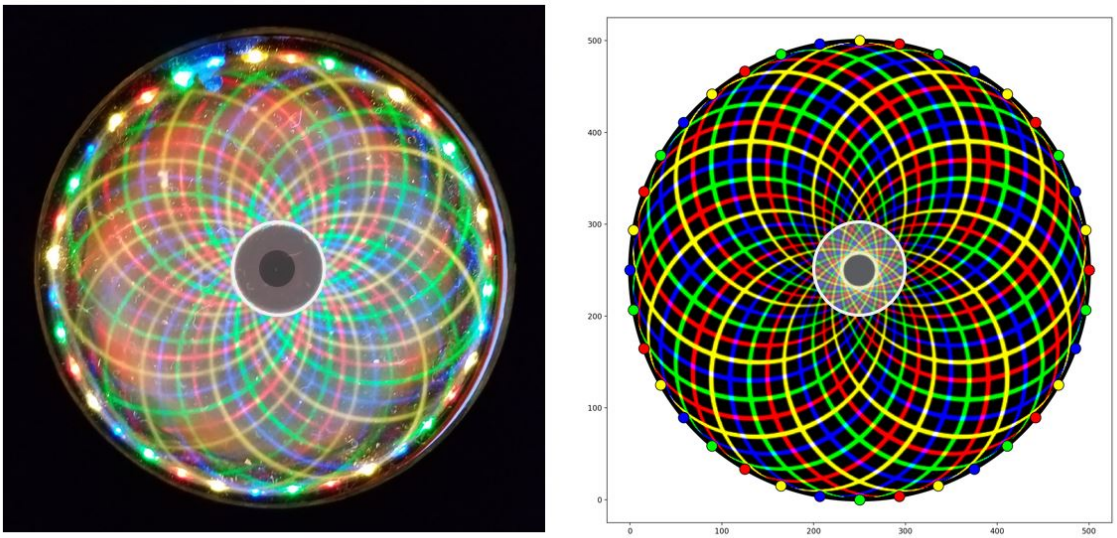

Figure 3: Left: Experimental setup. Cylinder magnet (d=h=10mm). Polar view. Ferrolens (d=5cm), 36 lights. Right: Simulation of experimental setup. The magnet is highlighted in grey.

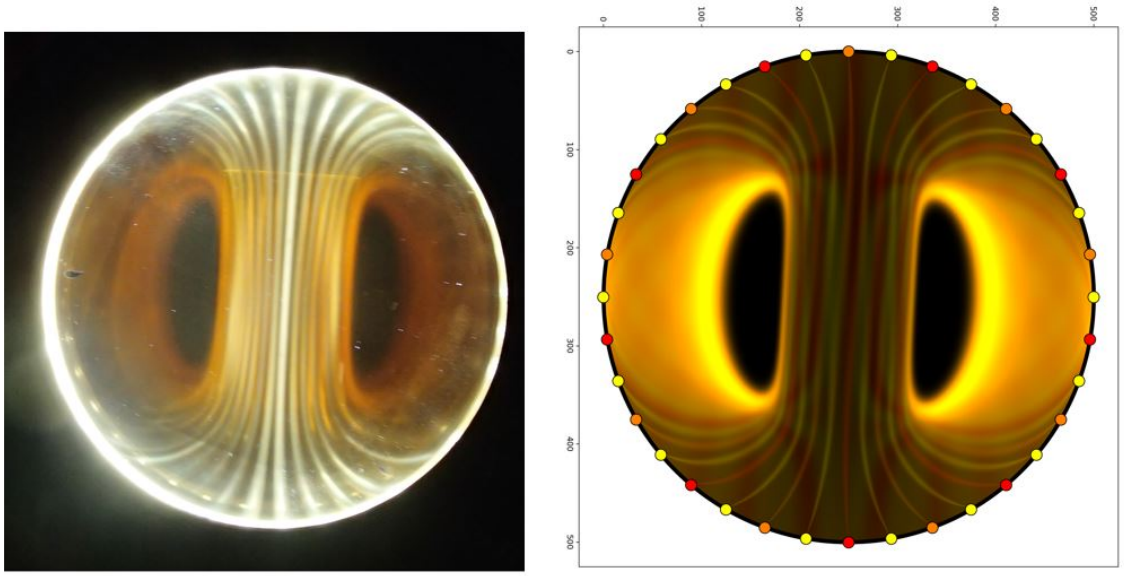

Figure 4: Left: Experimental setup. Cube magnet (l=2" w=2" h=1"), dipole view, 10cm ferrolens, 36 lights. Right: Simulation of experimental setup on left.

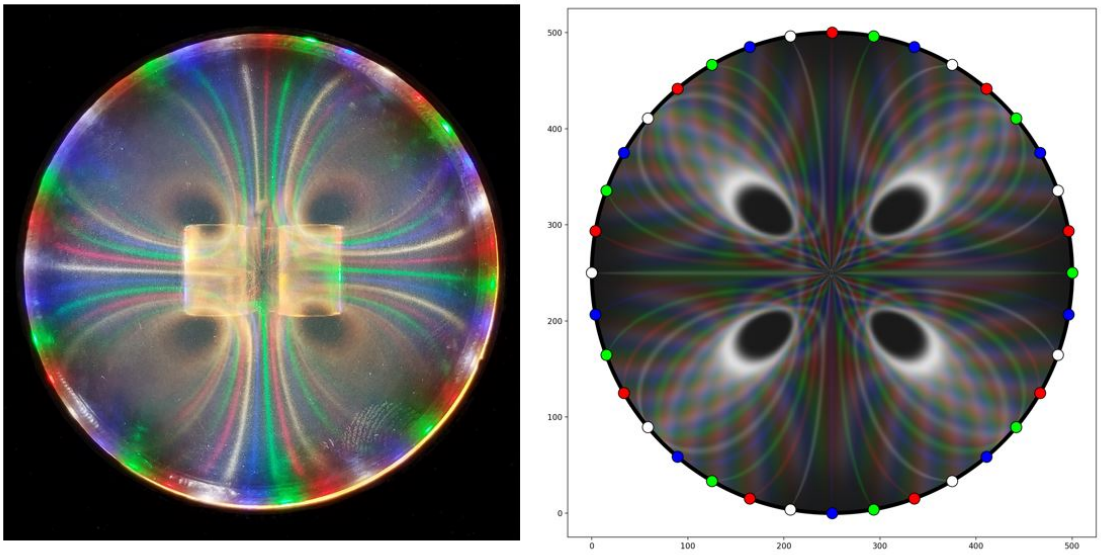

Figure 5: Left: Experimental setup. Two magnets (d=h=10mm). Side by side dipole view. Opposing poles, 5cm ferrolens, 36 lights. Right: Simulation of experimental setup.

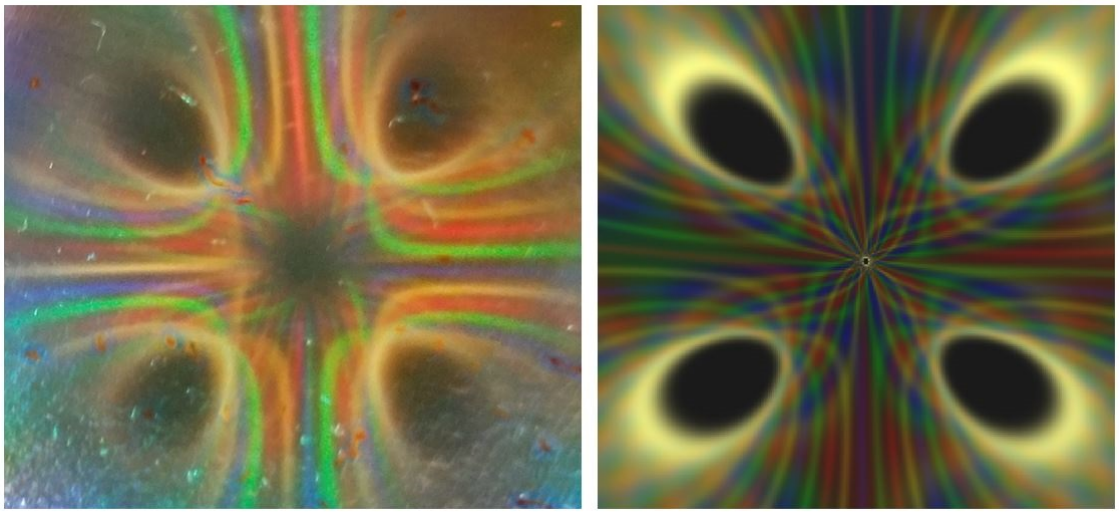

Figure 6: Left: Central region of ferrolens with magnet hidden and top glass removed. Right: Central region of simulation.

Figure 7 shows a close up of the crossing lines in both the ferrolens (left) and the simulation (right). As you can see, when the red lines and green lines intersect, yellow is observed; when green and blue intersect, cyan is observed; when red and blue intersect, magenta is observed and when yellow and blue intersect, white is observed. This is nothing other than additive colour mixing in standard light theory [8].

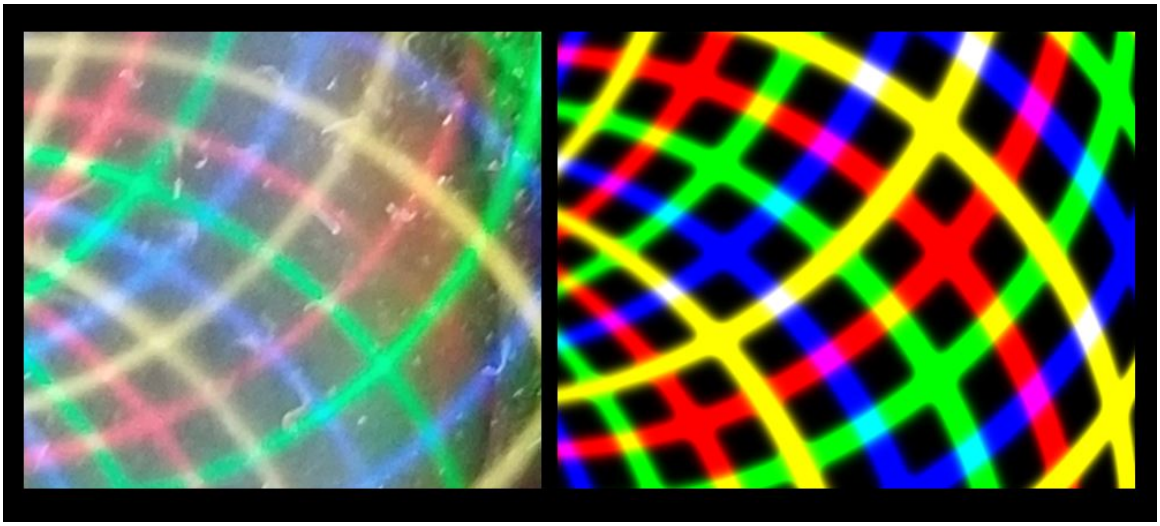

Figure 7: Left: Ferrolens close up to show colour mixing when lines cross. Right: Simulation showing similar colour mixing at the intersections of the crossing lines.

7 Discussion

Although the Ferrocell has been available since 2012 (Magnetic flux viewer, Patent Number: 8246356), a literature search will show that no computer simulation has yet been developed for this device. This is likely because of the confusion caused by the Ferrocell researchers in the field and the manner in which they describe the Ferrocell. For example, Vanderelli refers to his device as a "Magnetic Flux Viewer" in his patent which might give the false impression that the curved light lines that you see in the ferrolens correspond to magnetic flux lines. This might lead a computer scientist down the wrong garden path in terms of developing a simulation. Tufaile correctly identifies reflection as a potential cause of the Ferrocell patterns, however, in Figure 1 of his paper "Horocycles of Light in a Ferrocell" [5], a Ferrocell image is depicted next to a simulation of magnetic isopotentials [6] leading the reader to believe that the ferrocell is somehow displaying isopotentials. Although there are some similarities between these two images, there are not enough similarities to make a compelling argument. However, the simulation results presented in this paper do present compelling similarities with the ferrolens image compared to the isopotentials as can be seen in Figure 8. It should also be noted that the patterns seen in the ferrolens cannot be magnetic flux lines nor can they be isopotentials since crossing lines are often seen in the ferrolens and flux lines and iospotentials do not cross.

Although more work still needs to be done to perfect the simulation and colour displays, the author is confident that this is the correct approach to developing an accurate and functional Ferrocell

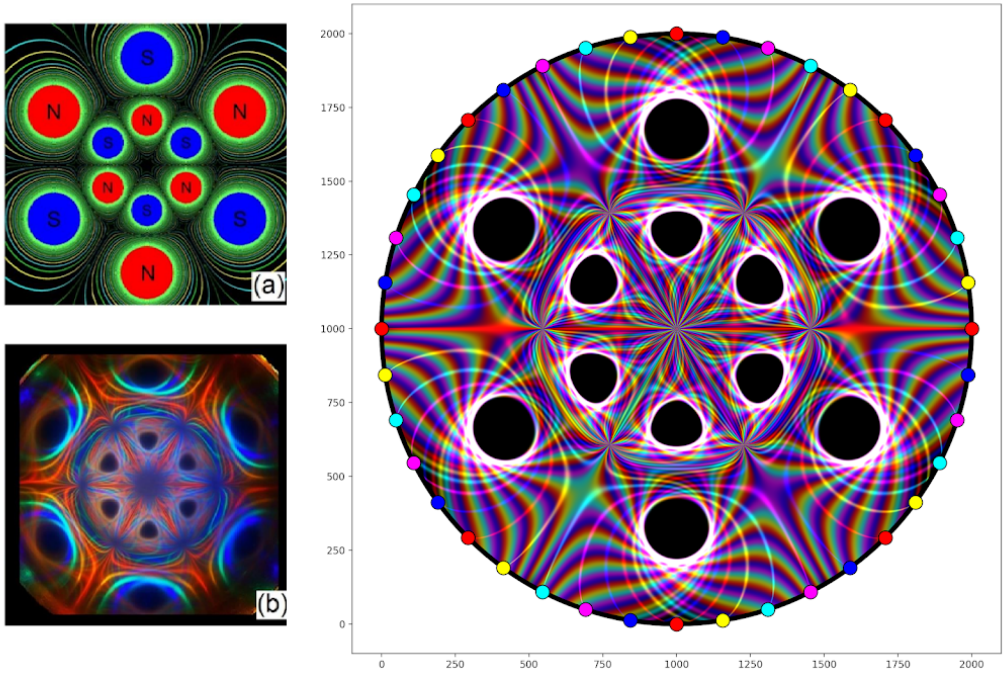

Figure 8: Upper left: 12 Magnet configuration with associated isopotentials. Lower left: Ferrocell image of 12 magnet configuration. Right: Simulation of 12 magnet configuration.

simulator.

8 Conclusion

Computer simulations were used to demonstrate that the interesting light patterns as seen in the Ferrocell are primarily caused by light reflections off the needle-like filaments that form and align with the magnetic flux lines of the magnet when placed in the vicinity of the ferrolens. All of the main features of the ferrolens display, including the paths of the light curves, the locations and shapes of the dark voids near the poles and the additive mixing of colours, are easily simulated using known laws of physics including the law of reflection, standard magnetic theory and standard light theory, thus demystifying the Ferrocell.

9 Acknowledgments

Special thanks to A.B. for the Python simulation code that made all of this possible. I would also like to thank László Vadkerti, for his images of ferrofluid under the microscope.

References

[1] Tufaile, Alberto, Timm A. Vanderelli, and Adriana Pedrosa Biscaia Tufaile. "Observing the jumping laser dogs." Journal of Applied Mathematics and Physics 4, no. 11 (2016): 1977-1988.

[2] Tufaile, Alberto, Michael Snyder, Timm A. Vanderelli, and Adriana Pedrosa Biscaia Tufaile. "Jumping Sundogs, Cat's Eye and Ferrofluids." Condensed Matter 5, no. 3 (2020): 45.

[3] Senior, T. B. A., and P. L. E. Uslenghi. "Experimental detection of the edge-diffraction cone." Proceedings of the IEEE 60, no. 11 (1972): 1448-1448.

[4] Keller, Joseph B. "Geometrical theory of diffraction." Josa 52, no. 2 (1962): 116-130.

[5] Tufaile, Alberto, Michael Snyder, and Adriana Pedrosa Biscaia Tufaile. "Horocycles of Light in a Ferrocell." Condensed Matter 6, no. 3 (2021): 30.

[6] `http://www.pic2mag.com/`

[7] Ortner, Michael, and Lucas Gabriel Coliado Bandeira. "Magpylib: A free Python package for magnetic field computation." SoftwareX 11 (2020): 100466.

[8] `https://en.wikipedia.org/wiki/Additive_color`